Biosensors and Bioelectronics 135 (2019) 224–230

Contents lists available at ScienceDirect

Biosensors and Bioelectronics

journal homepage: www.elsevier.com/locate/bios

Molecularly imprinted polymer-decorated signal on-off ratiometric electrochemical sensor for selective and robust dopamine detection

Jiao Yang[1], Yue Hu[1], Yingchun Li*

College of Science, Harbin Institute of Technology (Shenzhen), Shenzhen, Guangdong, 518055, PR China

ARTICLE INFO

Keywords:
Ratiometric electrochemical sensor
Molecularly imprinted polymers
Dopamine
Specificity
Robustness

ABSTRACT

Dopamine (DA), as one of the central neurotransmitters, plays an important role in many physiological and pathological processes. Detection of DA is critical to diagnose and monitor some neurological diseases. In this work, a novel on-off ratiometric electrochemical sensor with molecularly imprinted polymers (MIPs) as target molecule recognizer has been developed for selective and accurate detection of DA. Nanoporous gold (NPG) was electrodeposited on bare gold electrode, which not only benefited the output signal amplification, but also provided enlarged surface for immobilization of polythionine (pThi) and MIPs. Oxidation of DA and pThi served as response signal and internal reference signal, respectively. The oxidation peak currents of DA at +0.12 V increased with increasing the concentration of DA, while the peak currents of pThi at −0.2 V decreased simultaneously. Due to the specificity from MIPs and the built-in correction from pThi, the fabricated sensor showed excellent performance in view of selectivity and reproducibility. It's worth to mention that even if the surface area and morphology of working electrode underwent huge variation deliberately, the assay deviation among these ratiometric sensors was largely reduced around 10 times. The proposed sensor demonstrated a broad dynamic range of 0.3–100 μM, as well as a low detection limit of 0.1 μM (S/N = 3). Moreover, superior anti-interfering ability toward DA detection was obtained despite the presence of interferents at high concentration in artificial cerebrospinal fluid (aCSF). Therefore, this work is expected to provide an alternative pathway for constructing ratiometric electrochemical sensor and offer reliable determination of small molecules with high selectivity and stability.

1. Introduction

Dopamine (DA) has been verified as a key neurotransmitter in the central nervous system and a vital substance in cell impulse transmission(Heien et al., 2005). It conveys the message of excitement and happiness and plays an important role in many physiological and pathological aspects. The abnormal concentration of DA in human brain may not only cause some motor diseases but also lead to some neurological disorders, such as Parkinson's syndrome and schizophrenia (Perry et al., 2009; Tao et al., 2013). Therefore, it is significant to develop a rapid and accurate method to detect DA in complex physiological environments. So far, lots of methods have been successfully applied for DA detection, including chromatography(Wu et al., 2016), fluorometry(Suzuki and Yoshio. 2017), chemiluminescence analysis (Gao et al., 2017), colorimetry(Wen et al., 2016), and electrochemical assays(Xie et al., 2017). Owing to its high sensitivity and accuracy, low cost and simple operation, electrochemical technique is one of the most convenient and suitable way among various analytical methods. However, traditional electrochemical sensors suffer from very poor stability, reproducibility and robustness because of the hard-to-avoid extrinsic variations during fabrication and application processes. To solve this problem, introduction of an internal reference to prepare a ratiometric electrochemical sensor has received extensive attentions in recent years (Chai et al., 2013; Hanjun et al., 2015). The internal reference can provide built-in correction towards uncontrollable inherent influences caused by environmental and personal factors, presenting much more reliable results and enhancing stability and repeatability of sensor (Zhang et al., 2009). Generally, ratiometric electrochemical sensors are divided into two types: signal on/off and signal on-off. Compared with signal on/off type, the reference signal and the response signal changed oppositely towards target molecules in signal on-off type sensor. This means that, in signal on-off model, not only can result be corrected by introduction of internal reference, but also combination of dual signals can elevate sensitivity and eliminate analyte-independent interference

* Corresponding author. College of Science, Harbin Institute of Technology, Shenzhen, 518055, China.
E-mail address: liyingchun@hit.edu.cn (Y. Li).
[1] These authors contributed equally to this work.

https://doi.org/10.1016/j.bios.2019.03.054
Received 14 February 2019; Received in revised form 20 March 2019; Accepted 26 March 2019
Available online 29 March 2019
0956-5663/

that may occur in signal on/off type sensor(Jin et al., 2017).

Another drawback limits the practical application of electrochemical tactic in DA detection is the relatively low anti-interfering ability due to the fact that DA usually coexists with many kinds of electroactive substances and its concentration is much lower than others. Much effort has been made to improve selectivity in DA detection, one common strategy of which is to employ various agents such as carbon materials(Kim et al., 2010; Zhang et al., 2010), organic molecules(Shervedani et al., 2006), polymers(Chen et al., 2010; Rice and Nicholson, 1989) and their composites(Thiagarajan and Chen, 2008) for catalyzing electrochemical reaction of DA specifically. However, cross-interference can not be well circumvented(Zhang et al., 2012; Zimmerman and Wightman, 1991). Emergence of aptamer provides a high specific approach in detecting target molecules and electrochemical sensors based on aptamer with specific affinity for DA have also been reported(Zhang et al., 2010). Nevertheless, the inherent instability and high cost hinder the commercial application of these aptamer-based sensors. In addition, unlike biological macromolecules, cells and microorganisms, the simple structure of DA molecule results in few binding sites and weak affinity with aptamer(Smuc et al., 2013). By comparison, molecularly imprinted polymers (MIPs) are usually regarded as artificial antibody, which possess obvious advantages including specific recognition ability, inherent robustness, mechanical/chemical stability as well as low cost. At present, based on the above advantages of MIPs, many novel nanosensors have been constructed by combining MIPs with kinds of nanoparticles and quantum dots for the sensitive and specific detection of cardiac troponin-I(Yola and Atar, 2019), anticancer drug (Zaidi, 2019), Cypermethrin(Atar and Yola, 2018) and Casein(Ashley et al., 2018). In MIP-based electrochemical sensors, uniformity and thickness of MIP film can be finely monitored by adjusting electropolymerization conditions(Otero and Ariza, 2003). Therefore, involvement of MIP is expected to afford sensor with high specificity together with cost-effectiveness and stability(Jun, 2015; Mayes and Mosbach, 1997).

Herein, a signal on-off ratiometric electrochemical sensor based on MIPs has been developed for detection of DA by using nanoporous gold (NPG) as substrate. The internal reference-polythionine and the target molecule recognizer-MIPs were electropolymerized on the surface of NPG successively. After elution of the template (DA) from MIP membrane, a stable reference peak of polythionine appeared. With the rebinding of DA molecules, the oxidation peak of DA arose while the peak of polythionine decreased gradually. The constructed ratiometric MIP sensor exhibits an outstanding sensing performance in the aspects of selectivity, stability, reproducibility and reliability. Moreover, the sensor can be used to monitor DA in artificial cerebrospinal fluid (aCSF) despite the presence of several interferents.

2. Experimental

2.1. Chemicals and instruments

Dopamine (DA), uric acid (UA), ascorbic acid (AA), urea, D-(+)-glucose and *o*-aminophenol were obtained from Adamas Reagent Co. Ltd. (Shanghai, China). Thionine, pyrrole, *o*-phenylenediamine and resorcinol were purchased from Sigma-Aldrich (Shanghai, China). Gold acid chloride trihydrate ($HAuCl_4{\cdot}3H_2O$) was supplied by Alfa Aesar (Shanghai, China). Phosphate buffered saline (PBS, 0.1 M) as supporting electrolyte was prepared with KH_2PO_4 and K_2HPO_4, and the pH value was adjusted to 7.0 by using HCl solution. Artificial cerebrospinal fluid (aCSF) was prepared by dissolving NaCl (126 mM), KCl (2.4 mM), $CaCl_2$ (1.1 mM), $NaHCO_3$ (27.5 mM) and KH_2PO_4 (0.5 mM) into deionized water, and then glucose, urea, AA and UA were added with the concentration at 200 μM. Finally, pH value of the obtained solution was adjusted to 7.4 by adding 5 M HCl or 5 M NaOH. Other reagents, such as $K_3[Fe(CN)_6]$, $K_4[Fe(CN)_6]$ and $CuSO_4{\cdot}5H_2O$ were of analytical level and used as received. Deionized (DI) water was utilized in the whole experiments.

All electrochemical measurements were performed at room temperature on an electrochemical workstation (CHI 660E, Shanghai Chenhua, China). A conventional three-electrode system was employed with modified gold electrode as a working electrode, a platinum wire as a counter electrode, and Ag/AgCl (saturated KCl solution) as a reference electrode. Unless mentioned otherwise, all potentials were referred to the Ag/AgCl (saturated KCl solution). For electrochemical impedance spectroscopy (EIS) measurement, a sine wave of 10 mV amplitude was applied in a wide frequency range from 10 mHz to 100 kHz to the working electrode. Differential pulse voltammetry (DPV) was conducted from −0.5 to 0.5 V with a pulse amplitude, width and period of 50 mV, 100 ms and 16.7 ms, respectively. Surface morphology of the modified electrodes was characterized with a S-4800 field emission scanning electron microscope (FE-SEM, Hitachi, Tokyo, Japan). Attenuated total reflection infrared spectroscopy (ATR-IR) experiments were operated on a fourier transform infrared spectrometer (VERTEX70V, Brooke, Germany).

2.2. Preparation of NPG modified electrodes

Before modification, gold disk electrodes (diameter of 2 mm) were polished and cleaned according to the literature(Gui-Xia et al., 2012). Electrochemical preparation of NPG was referred to the modified Tominaka's method(Tominaka, 2011). Briefly, Au-Cu alloy was first electrodeposited in 0.5 M H_2SO_4 containing 10 mM $HAuCl_4$ and 10 mM $CuSO_4$ with applied potential of 0.15 V for 1000 s. Subsequently, dealloying of Cu was.

2.3. Fabrication of MIPs/pThi/NPG electrodes

Firstly, thionine (Thi) was polymerized on NPG electrode in 5 mM thionine solution (pH 6.0) by cyclic voltammetry (CV) from −0.4 V to 0.4 V with the scan rate of 0.1 V s^{-1} for 30 consecutive cycles. Afterwards, preparation of MIP film was performed by CV between −0.2 V–0.8 V in PBS containing DA and pyrrole. Subsequent operation was to extract the embedded DA from the MIP layer, which was realized by CV scanning in PBS in the range of −0.2 V–0.6 V for several cycles until the oxidation peak of DA vanished. The obtained electrode was defined as MIPs/pThi/NPG electrode. As a control, a non-ratiometric electrode (MIPs/NPG) was synthesized according to the above steps except electropolymerization of thionine. Additionally, for comparison, an electrode modified with non-molecularly imprinted polymers (NIPs) was fabricated by the same procedure except for addition of DA during pyrrole electropolymerization, which was named as NIPs/pThi/NPG electrode.

2.4. Electrochemical detection of DA

DPV was carried out recording to the peak currents from oxidation of DA (I_{DA}) and pThi (I_{pThi}), and their current ratio (I_{DA}/I_{pThi}) was calculated. The electrode was first immersed in DA solution for 2 min to allow full DA adsorption, followed by the current response was measured in PBS.

In order to investigate the practicability of MIPs/pThi/NPG sensor for real-time detection, DPV response of the sensor was directly tested in aCSF containing various concentration of DA. All tests were measured for at least three times.

3. Results and discussion

3.1. Preparation and characterization of MIPs/pThi/NPG electrodes

As shown in Scheme 1, the on-off ratiometric DA sensor was fabricated by three steps with NPG electrode as matrix. The thionine was firstly electropolymerized on NPG electrode as the reference, followed

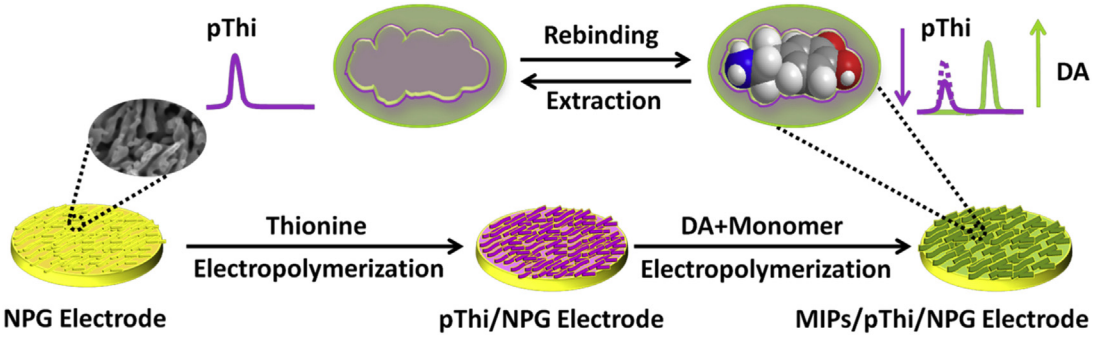

Scheme 1. Schematic diagram of the synthesis process of MIPs/pThi/NPG electrode carried out in 0.5 M H_2SO_4 at 1.0 V for another 2000 s. The obtained electrode was washed with water and denoted as NPG electrode.

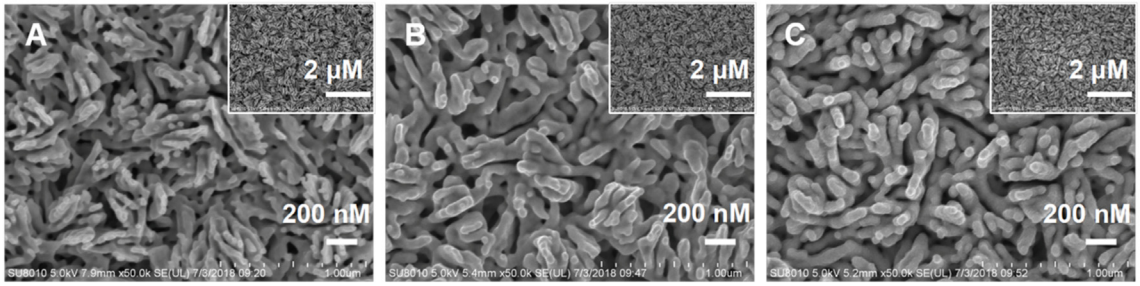

Fig. 1. SEM images of (A) NPG, MIPs/pThi/NPG (B) before and (C) after extraction of DA. Insets are the corresponding images at lower magnification.

by preparation of MIPs via electrochemical deposition and extraction. After removal of the template-DA from MIPs, the cavities in the polymer provide access for electrolyte to transfer onto the pThi layer, so the peak current of pThi appeared. While after rebinding of DA molecules, some of the cavities were occupied with DA, and thus the oxidation peak current of DA (I_{DA}) came out, in contrast, the peak current of pThi (I_{pThi}) decreased. The surface morphology of the prepared electrodes was characterized by FE-SEM. In Fig. 1A, NPG formed on bare gold electrode surface possesses spongelike structure with ligments of *ca.* 50–70 nm in width. By comparing the enclosed areas of CV curves (Fig. S1A), the real surface area of NPG electrode was 5.6 times larger than that of the bare gold electrode. After MIP deposition (Fig. 1B), the spongelike structure showed no change and only the width of ligments increased to *ca.* 80–100 nm, indicating that the polymer was successfully prepared. Moreover, after extraction of DA (Fig. 1C), the polymer membrane became rougher than before, which can be attributed to the structure transformation of polypyrrole during the elution procedure (Pandey et al., 2003).

The electrochemical behavior of each modification step was monitored by CV (Fig. 2A). The redox probe exhibited reversible redox peaks at the bare gold electrode; after NPG deposition, the redox peak currents increased significantly due to its enlarged electroactive surface area. Subsequent modification of pThi showed no change of the redox peaks, which is owing to the fact that the polymeric film is conductive and also thin enough to be favorable for the electron tunneling current. After decoration of MIPs on pThi/NPG electrode, the peak current remained constant and the shape of CV curve was similar to that of a capacitor, illustrating the DA-doped polypyrrole possesses the properties of capacitor with high conductivity(Zhang et al., 2016). At last, removing template molecules resulted in the appar-

Ent suppression of redox peak currents due to the conductivity decrease of polypyrrole caused by successive CV scanning.

Electrochemical impedance spectroscopy (EIS) was also carried out to verify each modification step of MIPs/pThi/NPG electrode. Impedance spectroscopy consists of a high frequency semicircular part corresponding to the limited process of electron transfer and a low frequency linear part associating with the diffusion controlled process. The electron transfer resistance (R_{et}) was calculated by measuring the diameter of the high-frequency semicircle. As shown in Fig. 2B, the small semicircle at bare gold electrode was obtained with impedance of 121.8 Ω. After electrodeposition of NPG, the R_{et} decreased apparently, which was attributed to the nanosized gold forming high electron conduction pathways. When NPG was successively modified with pThi and MIPs, the R_{et} was almost unchanged, originating from the excellent electron transport ability of pThi and polypyrrole. While after DA extraction, the resistance increased to 684.2 Ω, suggesting that the conductivity of polypyrrole is impaired during successive.

CV scanning. The EIS data were in good agreement with the CV data.

ATR-IR measurements were also tested to confirm successful construction of the expected electrodes (Fig. 2C). For NIPs/pThi/NPG electrode, a main absorption peak at 1050 cm^{-1} was assigned to the C-N stretching vibration in aromatic amine from polypyrrole, and the multiple peaks from 1537 cm^{-1}–1325 cm^{-1} were related to pyrrole backbone ring(Zamora-Gálvez et al., 2016). Regarding the spectra of MIPs-decorated electrode, the peaks at 935 cm^{-1} and 850 cm^{-1} were ascribed to C-H out-of-plane deformation vibration of 1,2,4-trisubst benzenes in DA(Lambert and Joseph, 1987), indicating that DA molecules were involved in MIPs during electropolymerization. After template molecules extraction, the above peaks corresponding to DA almost disappeared and only the peaks belonging to polypyrrole retained, demonstrating that DA molecules were removed from MIPs. Meanwhile, the broad band from 3200 cm^{-1}–4000 cm^{-1} was assigned to hydrogen bond formed during the removal of template molecules, which benefits the rebinding of DA into MIP membrane.

In order to clarify the imprinting effect on sensing performance, MIPs/pThi/NPG and NIPs/pThi/NPG electrodes were used to detect 75 μM DA in PBS. As shown in Fig. 2D, after DA rebinding, I_{DA} increase and I_{pThi} decrease occurred at both MIPs and NIPs modified electrodes. However, the ratio (I_{DA}/I_{pThi}) of MIP sensor was much higher than that from NIP sensor, implying the existence of imprinted cavities in MIP film and their selective recognition ability toward DA detection.

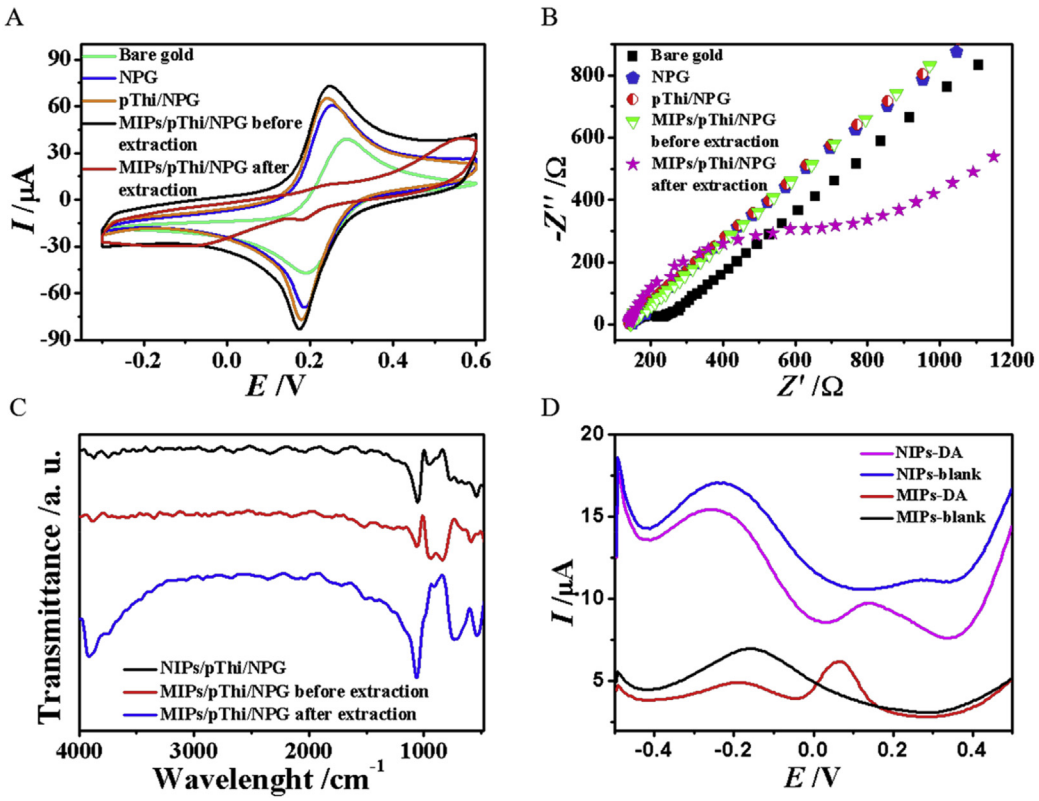

Fig. 2. (A) CV curves and (B) Nyquist diagrams of bare gold, NPG, pThi/NPG, MIPs/pThi/NPG electrodes before and after elution in 0.1 M KCl aqueous solution containing 5 mM $[Fe(CN)_6]^{3-/4-}$. Scan rate of 50 mV s^{-1}. (C) ATR-IR spectra of NIPs/pThi/NPG, MIPs/pThi/NPG electrodes before and after elution. (D) DPV responses of MIPs/pThi/NPG and NIPs/pThi/NPG electrodes in PBS before and after incubation of 75 μM DA. (For interpretation of the references to color in this figure legend, the reader is referred to the Web version of this article.)

3.2. Optimization of the parameters for MIPs preparation

As is known to all, optimizing the composition of MIPs is crucial for constructing MIPs sensors. On the one hand, MIPs should not hinder the electron transfer of the internal reference signal after extraction; on the other hand, it needs to satisfy the specific recognition and rebinding of template molecules. In order to maximize the performance of MIPs/pThi/NPG electrode on DA detection, the effects of some critical factors (i.e. functional monomer, pH value, the number of CV scanning cycles, and monomer/template ratio) were assessed. Firstly, four kinds of functional monomers (*o*-phenylenediamine, 2-aminophenol, resorcinol, and pyrrole) were tested and all these MIPs were prepared under the same conditions as described in Experimental Section. As shown in Fig. 3A, there was no or weak oxidation peak of pThi observed after DA extraction when 2-aminophenol, *o*-phenylenediamine and resorcinol as functional monomer. This phenomenon would be attributed to incomplete elution of template owing to the strong binding ability of these monomers toward DA. In contrast, MIPs formed with pyrrole as monomer exhibited high pThi peak current after DA elution. During CV scanning, polypyrrole was charged and discharged many times, causing the structure of MIPs looser and thus promoting the electron/mass transfer rate(Pandey et al., 2003). Therefore, pyrrole was selected as the functional monomer in the following experiment.

The effect of pH value on sensing response was investigated in the range from 5.0 to 9.0. In Fig. 3B, the value of I_{DA}/I_{pThi} increased sharply from pH 5.0 to pH 7.0, and then decreased dramatically, which could be ascribed to the fact that DA would lose its proton in alkaline condition, leading to weak interaction with functional groups in monomers. Thereby, the amount of embedded DA molecules in MIP is reduced and fewer recognition sites are generated after elution(Anirudhan et al., 2014). Therefore, the optimum pH value was set at 7.0. The thickness of MIPs also plays an important role as it affects the rebinding and recognition capacity of the sensor. In this study, the thickness of MIPs was controlled by adjusting the number of scanning cycles during electropolymerization. It was found that the I_{DA}/I_{pThi} response increased with the cycle number from 4 to 7 but reduced when it altered from 7 to 20 (Fig. 3C). The thinner film is, the less imprinted sites are. However, too thick MIPs film hinders complete removal of template molecules. The template residual reduced the accessible imprinted cavities and consequently resulted in low binding capacity and slow kinetics(Song et al., 2010). Hence, electropolymerization for 7 cycles was selected.

The monomer/template (M/T) ratio is another important factor which influences polymer structure and rebinding affinity. According to Fig. 3D, I_{DA}/I_{pThi} decreased with the increase of M/T ratio. It may be contributed to the fact that less DA molecules were involved in the formation of MIPs at higher M/T ratio, providing fewer recognition sites for the rebinding of DA molecules(Andersson et al., 2010). Moreover, based on charge-balance mechanism, more pyrrole could polymerize on electrode surface when embedded DA molecules serving as dopant in polypyrrole backbone(Wang et al., 2006). It's worth noting that although the highest response was obtained at M/T ratio of 0.5:1, some unexpected peaks appeared at this ratio (Fig. S1B). In summary, we chose 1:1 as the optimal M/T ratio.

3.3. Comparison of MIPs/pThi/NPG and MIPs/NPG electrode

In order to assess the advantages of the developed ratiometric electrochemical sensors (MIPs/pThi/NPG) over the sensors without internal reference (MIPs/NPG), we used three kinds of gold electrodes: one is unmodified electrode with diameter of 2 mm, the second and third are modified with NPG with diameter of 2 mm and 4 mm, respectively. Then they underwent the process of preparing ratiometric or non-ratiometric MIP sensor. The sensing performances of these sensors toward DA detection were investigated. As depicted in Fig. 4A, totally different response curves were observed when the three non-ratiometric electrodes with varied surface morphology and electroactive area were applied. In contrast, the response difference among the three ratiometric sensors was much less significant and the assay deviation was about 10 times lower than that of non-ratiometric sensors (Fig. 4B). This result revealed that introduction of the internal reference can

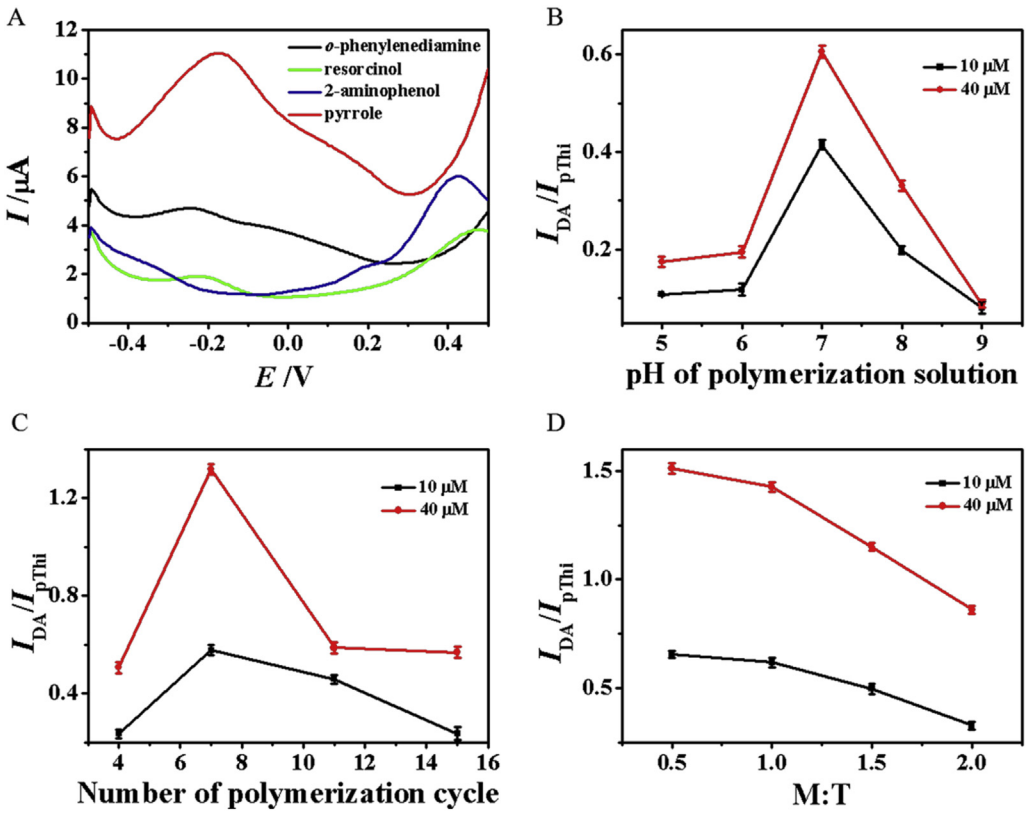

Fig. 3. (A) DPV responses of the MIPs/pThi/NPG electrode in PBS with different functional monomers: o-phenylenediamine, resorcinol, 2-aminophenol, and pyrrole. (B) The effects of pH value, (C) electropolymerization cycles and (D) M/T ratio on DPV responses of MIPs/pThi/NPG electrode subjected to incubation with 10 μM (black color) and 40 μM (red color) of DA. Error bars represent the standard deviation from three parallel tests. (For interpretation of the references to color in this figure legend, the reader is referred to the Web version of this article.)

greatly reduce these environmental and personal influences and improve robustness and reliability of electrochemical sensors a lot.

To further demonstrate the unique predominance of the proposed ratiometric electrochemical sensors, the sensing behaviors of MIPs/pThi/NPG electrodes and MIPs/NPG electrodes were compared by seven consecutive determinations. After each measurement, both electrodes were washed with DI water for 10 s and then the next test was carried out. In Fig. 4C, the IDA of MIPs/NPG electrode decreased with

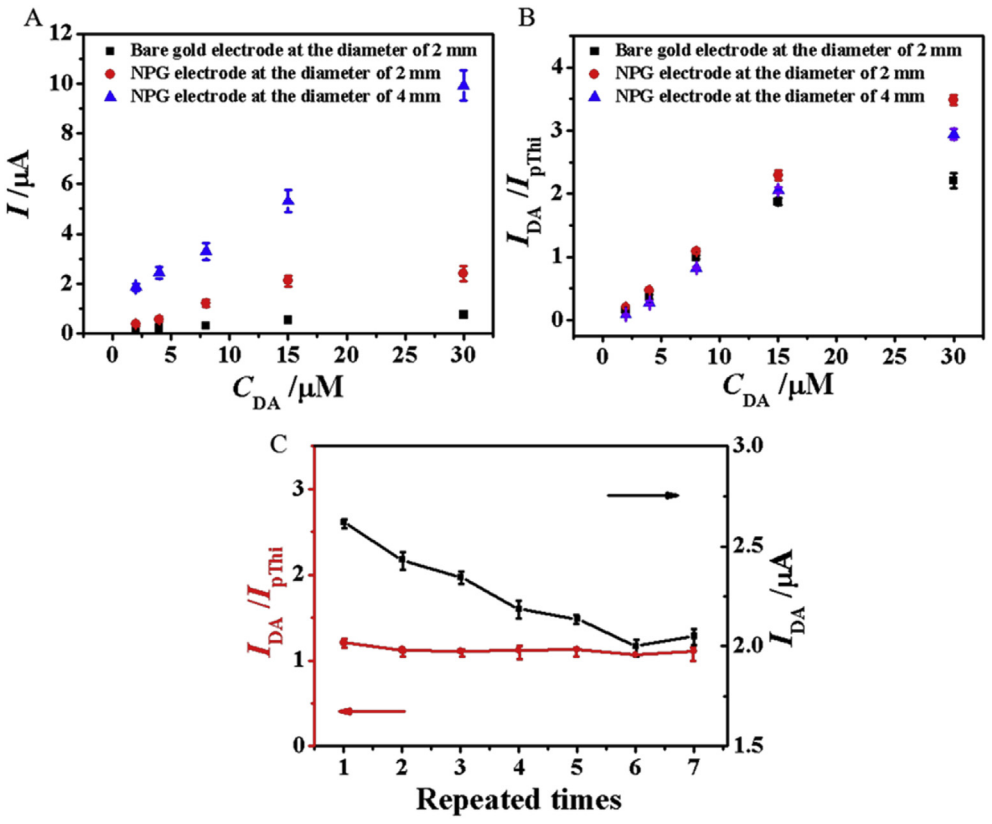

Fig. 4. Plots of electrochemical response versus DA concentration in aCSF by using (A) MIPs/NPG electrode and (B) MIPs/pThi/NPG electrode with different surface area. (C) Plots of electrochemical response versus repeating times with MIPs/pThi/NPG electrode (red color) and MIPs/NPG electrode (black color). Error bars represent the standard deviation from three parallel tests. (For interpretation of the references to color in this figure legend, the reader is referred to the Web version of this article.)

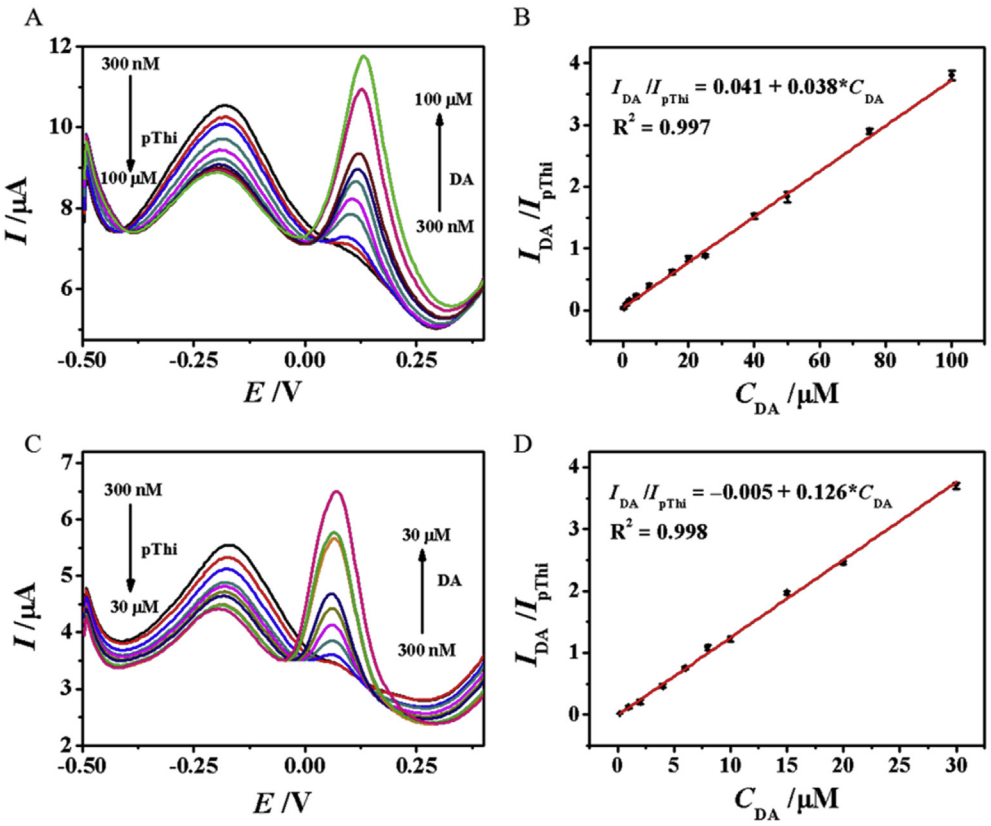

Fig. 5. (A) DPV responses and (B) calibration curve of MIPs/pThi/NPG electrode in PBS (pH = 7.0) after incubation of different concentrations of DA. (C) DPV responses and (D) calibration curve of the MIP sensor in aCSF containing various concentrations of DA. Error bars represent the standard deviation from three parallel tests.

the increase of assays, while for MIPs/pThi/NPG electrode, the ratio of the peak currents (I_{DA}/I_{pThi}) remained almost constant, providing further evidence concerning the more remarkable robustness and reliability of ratiometric electrochemical sensors over non-ratiometric sensors.

3.4. Assessment of DA sensor performance

The performance of MIPs/pThi/NPG based DA sensor was evaluated in view of dynamic detection range, selectivity, spike recovery and repeatability. Fig. 5A depicted DPV responses of MIPs/pThi/NPG electrode in PBS after the incubation of DA at various concentrations. One can observe that the I_{DA} (~0.12 V) increased with the increase of DA concentration, whereas I_{pThi} (~ −0.2 V) as internal reference decreased significantly. This result suggested that cavities in MIPs were occupied by DA molecules, which hindered the electron transfer of pThi layer. It was found that the MIPs/pThi/NPG sensor showed a wide linear relationship in the range of 0.3–100 μM, with the regression.

Coefficient of 0.997 (Fig. 5B). The detection limit was calculated to be 0.1 μM (S/N = 3). To assess the feasibility of proposed sensor for real-time detection, DPV was directly scanned in aCSF containing different concentrations of DA. As shown in Fig. 5C and D, similar DPV response curve were obtained in aCSF despite of several interferents on their physiological normal levels. A good linearity ranging from 0.3 μM to 30 μM was also obtain-

Ed with R^2 of 0.998. All above results suggested remarkable anti-interfering ability and practicality of the sensor in real-time detection.

The selectivity of MIPs/pThi/NPG electrode was further investigated by successively immersing MIP sensor in 50 μM AA, 50 μM UA, 50 μM urea, 1 mM glucose, and 20 μM DA solution to allow adsorption. As illustrated in Fig. 6A, the MIPs/pThi/NPG electrode showed outstanding affinity to DA but negligible reactivity to other species even though their concentrations were much higher than DA.

Repeatability was studied by detecting 10 μM DA in aCSF for 20 successive times (Fig. S5B), which yielded relative standard deviation (RSD) of 4.2%. The result indicated that the sensor had decent repeatability. For long-term stability, the modified electrode was stored dry at room temperature and measured 10 μM DA every five days. From Fig. 6B, there was no significant decrement in current response and 92.4% of the initial response was retained after 30 days. Summarily, thanks to the advantage of superior selectivity and stability of MIPs, excellent robustness and reproducibility of ratiometric sensor, the MIPs/pThi/NPG electrode can be used for rapid and efficient determination of DA and has promising potential in practical application.

Thereby, in order to appraise the practical applicability of the constructed sensor, recovery test was adopted to investigate accuracy and reliability of the fabricated sensor in the assay of simulated samples. As listed in Table 1, the spike recoveries of DA measured by MIPs/pThi/NPG electrode were found to be 98.7% ~ 101% with RSD less than 3.0% for three independent measurements, suggesting that the proposed DA sensor can be applied for actual samples crowed with many interfering substances.

4. Conclusion

In this work, we have successfully designed a signal on-off ratiometric electrochemical sensor for the reliable and selective detection of DA in complex physiological environment, in which the internal reference-polythionine and the target molecule recognizer-MIPs were electropolymerized on the surface of NPG successively. It is worth to mention that the inner polythionine not only can avoid analyte-independent interference, but also can increase the sensitivity due to its signal decrease after DA rebinding. Thanks to the specificity of MIPs and built-in correction of polythionine, the fabricated sensor was successfully utilized for detection of DA in aCSF even in the presence of interferent species at high concentrations in a fast, reproducible, and selective manner. With all these merits, the DA sensor proposed herein is expected to provide a versatile methodology for designing

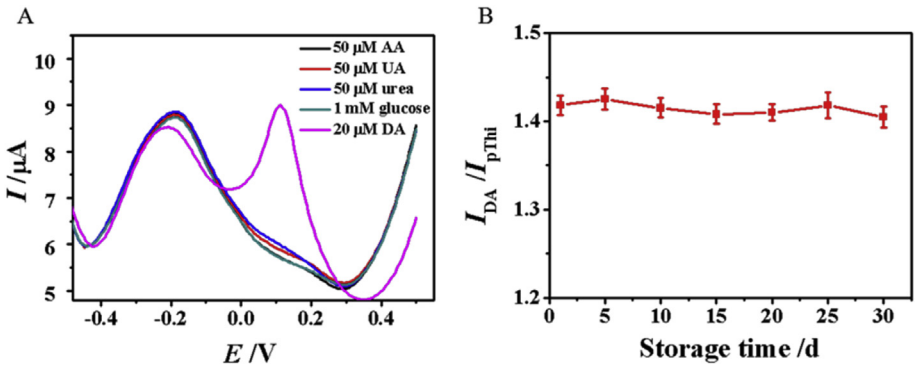

Fig. 6. (A) DPV responses of MIPs/pThi/NPG electrode in PBS after successive incubation in 50 μM AA, 50 μM UA, 50 μM urea, 1 mM glucose, and 20 μM DA solution. (B) Responses obtained from MIPs/pThi/NPG electrode in aCSF containing 10 μM DA after storage for various time periods. Error bars represent the standard deviation from three parallel tests.

Table 1
Spike recoveries of DA from PBS and aCSF (n = 3).

Sample	Determined (μM)	Spiked (μM)	Total found (μM)	Recovery (%)	RSD (%)
PBS	0	1	1.01 ± 0.03	101.0	2.97
		10	9.98 ± 0.12	99.8	1.20
		20	19.92 ± 0.33	99.6	1.66
aCSF	0	1	1.00 ± 0.02	100.0	2.00
		10	10.08 ± 0.28	100.8	2.78
		20	19.73 ± 0.47	98.7	2.38

electrochemical sensors with high selectivity and robustness for detection of other electroactive molecules. However, though stability is greatly enhanced by the ratiometric sensor, electrode fouling still exists and seriously impedes electron/mass diffusion. Tedious pretreatment is required in order to prolong the sensor life-span time. Thus, further study including introduction of self-cleaning materials and microfluidic chip are in progress to circumvent above issues.

CRediT authorship contribution statement

Jiao Yang: Methodology, Writing - review & editing. **Yue Hu:** Software, Data curation, Writing - original draft, Writing - review & editing. **Yingchun Li:** Writing - review & editing, Supervision.

Acknowledgments

The work financially supported by free exploration project from the Natural Science Foundation of Shenzhen (JCYJ20170811152540640).

Appendix A. Supplementary data

Supplementary data to this article can be found online at https://doi.org/10.1016/j.bios.2019.03.054.

Declaration of interests

The authors declare that they have no known competing financial interests or personal relationships that could have appeared to influence the work reported in this paper.

References

Andersson, H.S., Koch-Schmidt, A.C., Ohlson, S., Mosbach, K., 2010. J. Chromatogr. A 9 (5–6), 675–682.
Anirudhan, T.S., Alexander, S., Lilly, A., 2014. Polymer 55 (19), 4820–4831.
Ashley, J., Shukor, Y., D'Aurelio, R., Trinh, L., Rodgers, T.L., Temblay, J., Tothill, I.E., 2018. ACS Sens. 3 (2), 418–424.
Atar, N., Yola, M.L., 2018. J. Electrochem. Soc. 165 (5), H255–H262.
Chai, X., Zhou, X., Zhu, A., Zhang, L., Qin, Y., Shi, G., Tian, Y., 2013. Angew. Chem. Int. Ed. 125 (31), 8287–8291.
Chen, J., Zhang, J., Lin, X., Wan, H., Zhang, S., 2010. Electroanalysis 19 (5), 612–615.
Gao, W., Qi, L., Liu, Z., Majeed, S., Kitte, S.A., Xu, G., 2017. Sensor. Actuator. B Chem. 238, 468–472.
Gui-Xia, W., Wen-Jing, B., Min, W., Xing-Hua, X., 2012. Chem. Commun. 48 (88), 10859–10861.
Hanjun, C., Xiaoyu, W., Hui, W., 2015. Anal. Chem. 87 (17), 8889–8895.
Heien, M.L.A.V., Khan, A.S., Ariansen, J.L., Cheer, J.F., Phillips, P.E.M., Wassum, K.M., R Mark, W., 2005. P. Natl. Acad. Sci. USA. 102 (29), 10023–10028.
Jin, H., Gui, R., Yu, J., Lv, W., Wang, Z., 2017. Biosens. Bioelectron. 91, 523–537.
Jun, H., 2015. J. Sep. Sci. 32 (10), 1548–1565.
Kim, Y., Bong, S., Kang, Y., Yang, Y., Mahajan, R., Kim, J., Kim, H., 2010. Biosens. Bioelectron. 25 (10), 2366–2369.
Lambert, Joseph, B., 1987. Introduction to Organic Spectroscopy. MacMillan.
Mayes, A.G., Mosbach, K., 1997. Trac. Trends Anal. Chem. 16 (6), 321–332.
Otero, T.F., Ariza, M.J., 2003. J. Phys. Chem. B 107 (50), 13954–13961.
Pandey, S.S., Takashima, W., Kaneto, K., 2003. Thin Solid Films 438 (03), 206–211.
Perry, M., Li, Q., Kennedy, R.T., 2009. Anal. Chim. Acta 653 (1), 1–22.
Rice, M.E., Nicholson, C., 1989. Anal. Chem. 61 (17), 1805–1810.
Shervedani, R.K., Bagherzadeh, M., Mozaffari, S.A., 2006. Sensor. Actuator. B Chem. 115 (2), 614–621.
Smuc, T., Ahn, I.Y., Ulrich, H., 2013. J. Pharmaceut. Biomed. 81–82, 210–217.
Suzuki, Yoshio, 2017. Sensor. Actuator. B Chem. 239, 383–389.
Song, W., Chen, Y., Xu, J., Yang, X.R., Tian, D.B., 2010. J.Solid. State. Electr. 14 (10), 1909–1914.
Tao, Q., Shishan, W., Jian, S., 2013. Chem. Commun. 49 (41), 4610–4612.
Thiagarajan, S., Chen, S.M., 2008. Talanta 74 (2), 212–222.
Tominaka, S., 2011. J. Mater. Chem. 21 (26), 9725–9730.
Wang, J., Sun, X.L., Sun, X.J., Xiao, Y.H., 2006. Chemical Sensors.
Wen, D., Liu, W., Herrmann, A.K., Haubold, D., Holzschuh, M., Simon, F., Eychmüller, A., 2016. Small 12 (18), 2439–2442.
Wu, D., Xie, H., Lu, H., Li, W., Zhang, Q., 2016. Biomed. Chromatogr. 30 (9), 1458–1466.
Xie, L.Q., Zhang, Y.H., Gao, F., Wu, Q.A., Xu, P.Y., Wang, S.S., Gao, N.N., Wang, Q.X., 2017. Chin. Chem. Lett. 28 (1), 41–48.
Yola, M.L., Atar, N., 2019. Biosens. Bioelectron. 126, 418–424.
Zaidi, S.A., 2019. Analyst 144 (7), 2345–2352.
Zamora-Gálvez, A., Ait-Lahcen, A., Mercante, L.A., Morales-Narváez, E., Amine, A., Merkoçi, A., 2016. Anal. Chem. 88 (7), 3578.
Zhang, L., Zhou, H., Li, X., Lin, Y., Yu, P., Su, L., Mao, L., 2009. Electrochem. Commun. 11 (4), 808–811.
Zhang, W., Chai, Y., Yuan, R., Chen, S., Han, J., Yuan, D., 2012. Anal. Chim. Acta 756 (23), 7–12.
Zhang, W., Zhou, Y., Feng, K., Trinidad, J., Yu, A., Zhao, B., 2016. Adv. Electron. Mater. 1 (11) (n/a-n/a).
Zhang, Y., Pan, Y., Su, S., Zhang, L., Li, S., Shao, M., 2010. Electroanalysis 19 (16), 1695–1701.
Zimmerman, J.B., Wightman, R.M., 1991. Anal. Chem. 63 (1), 24.